

# Analysis of the ITER low field side reflectometer employing the Beam Tracing Method

A. Stegmeir\*, G.D. Conway, E. Poli, E. Strumberger

Max-Planck-Institut für Plasmaphysik, Boltzmanstrasse 2, D-85748 Garching bei München, Germany

## ARTICLE INFO

### Article history:

Received 25 March 2011

Received in revised form 22 July 2011

Accepted 25 July 2011

Available online 30 August 2011

### Keywords:

Beam tracing

Reflectometry

ITER

Field ripple

## ABSTRACT

The Beam Tracing Method, which describes electromagnetic wave propagation in the short wavelength limit including diffraction effects, is applied to microwave reflectometry. The TORBEAM code has been augmented with relativistic corrections to the electron mass – which are necessary for a reliable description in high temperature plasmas such as in ITER, and a beam coupling model for the receiving antenna coupling. The propagation and reception behaviour of reflectometer probe beams in the ITER geometry is computed. The received power is affected by the intensity of the beams, the offset of the beams respectively to the receiver antenna and the angle of incidence. Using a magnetic field derived from a 3D equilibrium it is shown that the effects of toroidal field ripple in ITER on the beam propagation are negligible. Various antenna configurations for the ITER low field side reflectometer are proposed and analyzed, particularly their sensitivity to plasma height variations.

© 2011 Elsevier B.V. All rights reserved.

## 1. Introduction

Microwave reflectometry is a widely used diagnostic technique for studying magnetically confined plasmas. A microwave/millimeter-wave beam is launched into the plasma (usually perpendicular to the confining magnetic field and parallel to the density gradient) where it propagates until it reaches the cutoff condition (where the plasma refractive index goes to zero) and is reflected. The refractive index depends on the probing microwave frequency  $\omega$ , the plasma density  $n_e$ , and (for X-mode polarization) the magnetic field  $B$ , and hence different parts of the plasma can be probed by varying the microwave frequency. By measuring the phase delay of reflected beam information on the radial profile of the electron density and its fluctuations can then be obtained [1,2].

On ITER several reflectometer diagnostic systems are being developed to measure the edge and core density profiles, the density fluctuations as well as the plasma position and rotation [3,4]. The primary system is the so-called Low-Field-Side Reflectometer (LFSR) system which consists of several reflectometers probing the plasma mid-plane from the tokamak outer, or low magnetic field side. The LFSR system design has evolved steadily in recent years [4–7]. The most challenging aspect of the system is the design of the ‘front-end’ components – the antennas and waveguide transmission lines which will be installed

in the vacuum vessel port-plug. The number of antennas, their position, orientation and size (i.e. gain) will critically affect the diagnostic’s ability to meet the measurement requirements [4]. Hence careful design of these components, based principally on simulation studies, will be crucial to the success of the diagnostic.

In this paper a detailed investigation of the basic behaviour of the beam propagation dependence on the antenna parameters is presented using the TORBEAM beam tracing code (which includes diffraction effects and relativistic corrections) with simulated ITER magnetic equilibrium and density and temperature profiles. Several possible antenna configurations are investigated using the beam tracing code coupled with antenna power coupling calculations. This allows a much more rigorous assessment and comparison of their relative performance and merits than was previously available [7].

The paper begins with a description of the computational model used, including the modeling of the launched beam, a background to the beam-tracing equations, and the formulation of the beam coupling efficiency from which the received power is calculated. An outline of the LFSR operational range together with details of the ITER configuration then follow. The criteria for the assessment exercise are then presented. The results are divided into two sections: first the basic behaviour of a single launched microwave probe beam is described and how it depends on the plasma geometry and the launch antenna parameters. Next, a detailed assessment of specific transmit (launch) and receive antenna configurations, such as monostatic, bistatic, hybrids, antenna arrays and their variations, is presented.

\* Corresponding author. Tel.: +49 89 32992018; fax: +49 89 32992580.  
E-mail address: [stegmeia@ipp.mpg.de](mailto:stegmeia@ipp.mpg.de) (A. Stegmeir).

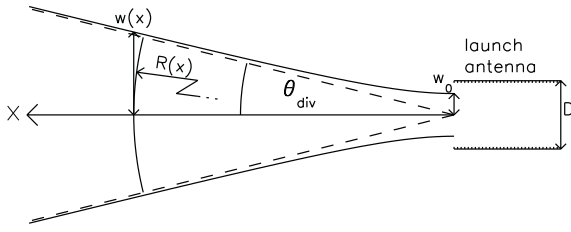


Fig. 1. Launch of Gaussian beam from corrugated waveguide.

## 2. Computational model

### 2.1. Modeling of launched beam

The ITER LFSR system will use circular aperture type antennas embedded into the equatorial port-plug blanket module. The antennas will be fed by low-loss oversized corrugated circular waveguide supporting the  $HE_{11}$  waveguide mode [8]. This mode couples in to an Gaussian beam antenna radiation pattern after a short distance ( $\approx 1/3 \cdot$  Rayleigh length, compare Fig. 2 in [9]). Fig. 1 shows the behaviour of the beam. In this frame, the normalized wave-function of the launch/receiver antenna radiation pattern  $\chi$  follow from the vacuum solution for Gaussian beams:

$$\chi(\vec{r}) = \frac{\sqrt{2/\pi}}{w_\chi(x)} \exp \left[ -iKx - i\frac{K}{2} \frac{y^2 + z^2}{R_\chi(x)} - \frac{y^2 + z^2}{w_\chi^2(x)} \right], \quad (1)$$

where the beam width, which is the radius of the  $1/e^2$  contour of the intensity cross-section, and phase front curvature are [10]:

$$w(x) = w_0 \left[ 1 + \left( \frac{x}{x_R} \right)^2 \right]^{1/2}, \quad R(x) = x \left[ 1 + \left( \frac{x_R}{x} \right)^2 \right], \quad (2)$$

with  $x$  the distance from the antenna and  $x_R = w_0^2 \omega / 2c$  the Rayleigh length and  $K = \omega/c$  the absolute value of the wavevector. The phase-front radius of curvature at the antenna aperture is usually given by the slant length of the antenna horn [10]. For the ITER antennas the slant length will be very long, so a good approximation is to set the phase-front curvature at the antenna aperture to infinity (i.e. flat phase-front). Hence the waist of the launched beam, which is given by  $w_0 = 0.32D$ , is directly at the antenna aperture. At large distances  $x \gg x_R$  the following approximations hold:

$$w(x) \approx x \tan \theta_{div}, \quad R(x) \approx x, \quad (3)$$

with the divergence angle  $\tan \theta_{div} = 2c/\omega w_0$ . Thus, after a few Rayleigh lengths the size of the cross-section is determined by the divergence angle. The lower the frequency and the smaller the diameter of the antenna the larger the cross-section.

### 2.2. Beam tracing

The propagation of the Gaussian beam through the plasma is calculated using the beam tracing approach [11,12]. Beam tracing is superior to ray-tracing [13,14] since it retains diffraction effects, and yields an analytic expression for the electric field across the beam profile, which is also possible, but not straightforward with ray-tracing [15]. Beam tracing is also computationally fast compared to full-wave simulations, since only ordinary differential equations need to be solved instead of partial ones.

Beam tracing gives an approximate solution of the Maxwell equations in weakly inhomogeneous media for wave-beams satisfying the condition:

$$\lambda \ll w \ll L, \quad (4)$$

where  $\lambda$  is the probing wavelength and  $L$  the typical inhomogeneity scale length of the medium. In the beam tracing solution the

propagation of the wave is described by a central ray, which obeys the same laws as in geometric optics:

$$\frac{dq_\alpha}{d\tau} = \frac{\partial H^M}{\partial k_\alpha}, \quad \frac{dK_\alpha}{d\tau} = -\frac{\partial H^M}{\partial x_\alpha}, \quad (5)$$

where  $q_\alpha$  is the trajectory of the central ray,  $K_\alpha$  the wavevector of the central ray and  $H^M$  a solution of the dispersion function:

$$\det \left[ \frac{c^2}{\omega^2} (-k^2 I + \vec{k}\vec{k}) + \epsilon^h \right] = 0, \quad (6)$$

with  $\epsilon^h$  the hermitian part of the dielectric tensor. In this work the anti-hermitian part is assumed to be zero, i.e. there is zero absorption.  $\alpha$  (and  $\beta, \gamma$ ) are indexes over the  $x, y$ , and  $z$  coordinates.

The electric field is expressed in terms of a complex phase  $\bar{s}(\vec{r}) = s(\vec{r}) + i\phi(\vec{r})$ :

$$\vec{E}(\vec{r}) = \vec{A}(\vec{r}) e^{i\bar{s}(\vec{r}) - \phi(\vec{r})}. \quad (7)$$

where  $s(\vec{r})$  describes the phase of the beam and  $\phi(\vec{r})$  describes a Gaussian cross-section. The scale ordering in condition (4) allows a paraxial expansion, i.e.  $s(\vec{r})$  and  $\phi(\vec{r})$  are expanded up to second order around the central ray:

$$s(\vec{r}) = s_0(\vec{r}) + K_\alpha [x_\alpha - q_\alpha] + \frac{1}{2} s_{\alpha\beta} [x_\alpha - q_\alpha][x_\beta - q_\beta], \quad (8)$$

$$\phi(\vec{r}) = \frac{1}{2} \phi_{\alpha\beta} [x_\alpha - q_\alpha][x_\beta - q_\beta]. \quad (9)$$

The matrix  $s_{\alpha\beta}$  and the positive definite matrix  $\phi_{\alpha\beta}$  have been introduced, where the complex quantity  $\bar{s}_{\alpha\beta} = s_{\alpha\beta} + i\phi_{\alpha\beta}$  obeys a complex matrix Riccati differential equation:

$$\frac{d\bar{s}_{\alpha\beta}}{d\tau} = - \left( \frac{\partial^2 H^M}{\partial x_\alpha \partial x_\beta} + \frac{\partial^2 H^M}{\partial x_\beta \partial k_\gamma} \bar{s}_{\alpha\gamma} + \frac{\partial^2 H^M}{\partial x_\alpha \partial k_\gamma} \bar{s}_{\beta\gamma} + \frac{\partial^2 H^M}{\partial k_\gamma \partial k_\delta} \bar{s}_{\alpha\gamma} \bar{s}_{\beta\delta} \right) \Bigg|_{\substack{x_\alpha = q_\alpha \\ k_\alpha = K_\alpha}}. \quad (10)$$

The second order expansion parameter of Eq. (8), the matrix  $s_{\alpha\beta}$ , is related with the curvature radius  $R$  of the phase front and the second order expansion parameter of Eq. (9), the matrix  $\phi_{\alpha\beta}$ , is related with the width  $w$  of the beam, at which the intensity of the beam drops to  $1/e^2$  compared to the intensity at the central ray:

$$s_{\alpha\beta} \sim \frac{\omega/c}{R}, \quad \phi_{\alpha\beta} \sim \frac{2}{w^2}. \quad (11)$$

Analytic solutions of the beam tracing equations in a slab model are presented in [16–18].

The TORBEAM code [20] solves the beam tracing equations numerically in a tokamak geometry with experimentally prescribed magnetic equilibria, density and temperature profiles. TORBEAM uses the cold plasma approximation of the dielectric tensor to calculate the beam trajectory and has implemented a generalized Snell's law [21] to take into account the transition at the vacuum plasma boundary. In ITER relativistic effects are expected to be important due to the high core electron temperatures. This was incorporated into the code using a simple, but well established, approximation of an effective electron mass in the cold dielectric tensor [22]:

$$m_{\text{eff}} = m_0 \left( 1 + 5 \frac{k_B T_e}{m_0 c^2} \right)^{1/2}, \quad (12)$$

where  $m_0$  is the rest mass of the electron,  $k_B$  the Boltzmann constant,  $T_e$  the electron temperature and  $c$  the speed of light. This approximation is in line with other models (e.g. [23]) and is sufficient for our investigations which are mainly constrained to the cooler ( $T_e \leq 5$  eV) pedestal region. Mazzucato [22] has also demonstrated that this approximation describes well the relativistic effects on beam propagation to the cutoff. For ITER core probing a fuller relativistic correction model may be required.

Download English Version:

<https://daneshyari.com/en/article/272423>

Download Persian Version:

<https://daneshyari.com/article/272423>

[Daneshyari.com](https://daneshyari.com)